

Comparisons of Measured Rate Constants with Spectroscopically Determined Electron-Transfer Parameters[†]

Stephen F. Nelsen,* Asgeir E. Konradsson, and Michael N. Weaver

Department of Chemistry, University of Wisconsin, 1101 University Avenue, Madison, Wisconsin 53706-1396

Rachel M. Stephenson, Jenny V. Lockard, and Jeffrey I. Zink*

Department of Chemistry and Biochemistry, University of California, Los Angeles, California 90095

Yi Zhao*

Department of Chemical Physics, University of Science and Technology of China, Hefei 230026, People's Republic of China

Received: December 29, 2006; In Final Form: February 13, 2007

This work involves comparison of rate constants measured for an intervalence (IV) compound with electron-transfer parameters derived from its optical absorption spectrum. The temperature-dependent rate constants for the radical cation having 3-*tert*-butyl-2,3-diazabicyclo[2.2.2]oct-2-yl (hydrazine) charge-bearing units attached para to a tetramethylbenzene bridge ($\mathbf{1}^+$) were previously measured. In this study, resonance Raman is used to calculate the magnitudes of the distortions of normal modes of vibration caused by excitation into the intervalence absorption band. These data produce a vibrational reorganization energy $\lambda_{\text{v}}^{\text{sym}}$ of 9250 cm^{-1} , and averaged single-mode ω_{v} for use in the Golden Rule equation of 697 cm^{-1} . Zhu–Nakamura theory has been used to calculate preexponential factors for analysis of the previously measured variable temperature optical spectra using quartic-enhanced intervalence bands to extract the total reorganization energy and the intramolecular electron-transfer rate constants for intramolecular electron transfer using electron spin resonance. In contrast to using the Golden Rule equation, separation of λ into solvent and vibrational components is not significant for these data. The Zhu–Nakamura theory calculations produce $\ln(k/T)$ versus $1/T$ slopes that are consistent with the experimental data for electronic couplings that are somewhat larger than the values obtained from the optical spectra using Hush's method.

Introduction

The comparison of electron-transfer rate constants measured for an intervalence (IV) compound by using electron spin resonance (ESR) methods with calculated rate constants based upon electron-transfer parameters derived from spectroscopy is the focus of this paper. IV compounds have charge-bearing units (M) connected by a bridge (B) and are at an oxidation level that would allow the charges on the M groups to be different. IV compounds that have their extra charge almost localized on one of the M groups, a $^+\text{M}-\text{B}-\text{M}$ charge distribution for a +1 charged system, are called class II in Robin and Day's nomenclature.¹ They are the simplest electron transfer (ET) systems ever devised, and they have remained important in ET studies since Creutz and Taube published the first designed example of an IV compound in 1969, the Creutz–Taube complex ($\text{M} = \text{Ru}(\text{NH}_3)_5$, $\text{B} = \text{pyrazine}$ (1,4-diazabenzene), charge +5).^{2–4} Hush had already pointed out that the longest wavelength absorption maximum for class II intervalence compounds is the total reorganization energy λ (assuming parabolic diabatic surfaces) and showed how to evaluate the electronic coupling V_{ab} from the intensity of this band (assuming that the ET distance is known).^{5,6} Completely organic examples of delocalized (Robin–Day class III) IV compounds have been known since the 19th century: the first radical ions ever isolated,

including Wurster's blue (*N,N,N',N'*-tetramethyl-*p*-phenylenediamine radical cation perchlorate),⁷ are examples, but organic chemists did not develop the idea that it would be useful to think about the possibility of charge localization in such systems.⁸ Completely organic class II intervalence compounds have also been made, starting with dinitrogen-centered ones.⁹ These compounds have much larger λ values than previously studied compound types, allowing study of compounds having large enough V_{ab} values for their IV absorption bands to be easily measured. By tuning λ and V_{ab} by changing the bridge, examples have been prepared that have intramolecular ET rate constants k_{et} near the 10^8 s^{-1} that corresponds to the point of maximum broadening for the nitrogen hyperfine ESR splitting, allowing accurate rate constant determination.^{10,11} These studies allow testing of methods for evaluating ET parameters and calculating rate constants. This work led to the rather unsatisfactory result that simple, classical Marcus theory that ignores a quantum mechanical treatment of molecular vibrations^{12,13} predicted the observed k_{et} more accurately than more sophisticated methods that incorporated such a treatment.¹⁴ It is the goal of this work to accurately establish the proper vibrational analysis of $\mathbf{1}^+$, which we have argued has the most accurately determined k_{et} as a function of temperature of the compounds that we have studied,¹⁵ because it has less spin density on the bridge than other cases. Resonance Raman has been used to establish the

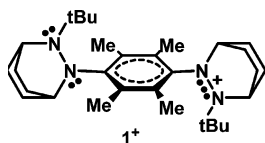
[†] Part of the special issue "Norman Sutin Festschrift".

TABLE 1: Resonance Raman Modes Excited by Irradiation into the IV Band of 1^+ ^a

ω_q	Δ_q	λ_q	λ_q/λ_v
435	2.89	1817	0.197
469	3.50	2875	0.311
506	2.44	1506	0.163
583	0.95	263	0.028
674	0.93	292	0.031
748	1.78	1185	0.128
1000	0.19	18	0.002
1163	0.82	391	0.042
1242	0.90	503	0.054
1404	0.34	81	0.009
1550	0.64	317	0.034

^a The energies are in cm^{-1} .

vibrations excited by irradiation into its IV band, and the experimental rate constants are compared with theory.



Results and Discussion

Resonance Raman Spectroscopy. Resonance Raman spectroscopy allows independent determination of both the vibrational frequencies of the modes, ω_q , that are distorted upon photoexcitation and the magnitudes of the relative distortions. Mode-specific reorganization energies λ_q are equal to one-half the product of the frequency and the square of the dimensionless distortion, Δ_q . These methods have been applied to many intra- and intermolecular electron-transfer systems including both inorganic (transition metal complexes),^{16–30} and organic compounds,^{31–35} and heterogeneous ET reactions.^{36,37} Resonance Raman studies on delocalized intervalence compounds include our study on a protected tetralkylamino-*p*-phenylenediamine radical cation,³⁸ a study of its tetraphenyl analogue,³⁹ and studies of two diarylhydrazine radical cations.^{40,41}

The normal modes ω_q and their dimensionless distortions Δ_q excited by irradiating into the IV band of 1^+ are shown in Table 1 along with their increments contributing to the total vibrational reorganization energy $\lambda_v = \sum \lambda_q$. All of the modes that contribute 1% or more reorganization energy as that of the most important mode (469 cm^{-1}) are included. Although weak Raman bands were observed in the CH region, much of their intensity arises from the nonresonant contributions to the scattering and have been ignored here because they are not expected to significantly contribute to ET. Each mode is fit numerically, and the intensity of the mode is the area of the fitted peak. The intensities are normalized to a standard nitrate peak at 716 cm^{-1} measured simultaneously with the sample. The relative Δ_q values are calculated from the normalized intensities using eq 1

$$\frac{I_k}{I_{k'}} = \frac{(\Delta_k^2 \omega_k^2)}{(\Delta_{k'}^2 \omega_{k'}^2)} \quad (1)$$

where k represents a mode of 1^+ and k' represents the standard nitrate mode (with a relative $\Delta_{k'}$ of 1).^{42–50} Equation 1 assumes that the potential surfaces are harmonic, that there is no change in force constant between the ground and excited states, and that the Condon approximation is valid. The values of each of the individual Δ_q values are determined from the relative Δ_q values by fitting the optical absorption spectrum using the

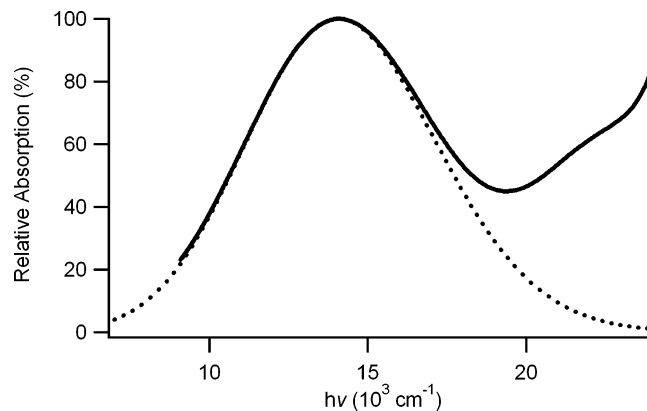


Figure 1. Simulation of the shape of the absorption spectrum of 1^+ using the modes of Table 1 and $\Gamma = 1300 \text{ cm}^{-1}$ (dashed) superimposed on the observed absorption spectrum at 252 K in acetonitrile.

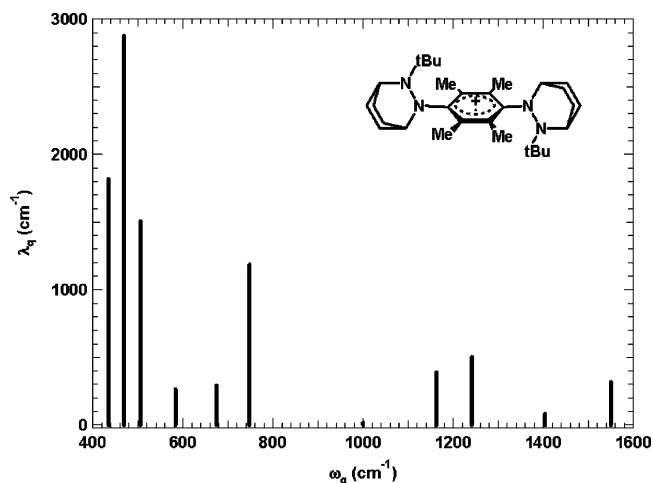


Figure 2. Mode-by-mode contributions to λ_v for Hy_2DU^+ .

time-dependent theory of spectroscopy. The experimental and calculated spectra are shown in Figure 1. For absorption, the time-dependent theory of spectroscopy uses eq 2

$$I(\omega) = C\omega \int_{-\infty}^{+\infty} \left\{ \langle \Phi | \Phi(t) \rangle \exp\left(-\Gamma^2 t^2 + \frac{iE_0}{h} t\right) \right\} dt \quad (2)$$

to find the intensity I at a frequency ω . In this model, Γ is a phenomenological damping factor that includes relaxation into other modes and the bath, and E_0 is the origin of the electronic transition. The Δ_q values are part of $\langle \Phi | \Phi(t) \rangle$, the autocorrelation function between the initial ground state wave packet and that wave packet over time as it moves in the excited state after the electronic transition. The modes are uncorrelated with each other, and thus $\langle \Phi | \Phi(t) \rangle$ is the product of the contributions of each of the individual vibrational modes. The increments to λ_v for each mode are given by $\lambda_q = \frac{1}{2} \omega_q \Delta_q^2$, and these values are shown in Table 1. Figure 2 shows the distribution of the λ_q modes, which sum to $\lambda_v = 9250 \text{ cm}^{-1}$ (26.4 kcal/mol), that if equated with λ_v would make $\lambda_s(\text{CH}_3\text{CN}) = 4850 \text{ cm}^{-1}$ (14.9 kcal/mol) because the total λ is 14 100 cm^{-1} (40.3 kcal/mol). The contributions to λ_v are dominated by low-frequency bending and twisting motions: 67% of λ_v arises from modes $\leq 506 \text{ cm}^{-1}$, 73% from those $\leq 674 \text{ cm}^{-1}$, and 86% $\leq 748 \text{ cm}^{-1}$.

A completely independent separation of λ_s and λ_v for 1^+ was achieved by study of shifts in the intervalence band maximum as a function of solvent.⁵¹ The values obtained in this manner are $\lambda_v = 10\,100 \text{ cm}^{-1}$ (28.9 kcal/mol) and $\lambda_s(\text{CH}_3\text{CN}) = 4000 \text{ cm}^{-1}$ (11.5 kcal/mol), that is, the present resonance Raman

study gives λ_v as 66% of the optical transition energy, while the solvent effect on the optical transition energy gave a λ_v contribution of 72%, which is remarkably good agreement.

The single-mode ω_v necessary for use with the Golden Rule equation (discussed below) should be the root-mean-square weighted average of the modes involved, which we calculated using $\omega_v = [\sum_q (\lambda_v^{\text{sym}}/\lambda_v)(\omega_v)^2]^{1/2}$,⁵² producing 697 cm^{-1} using the data of Table 1. This value is somewhat smaller than the 800 cm^{-1} we have used previously for Golden Rule equation rate constant calculations on Hy-centered hydrazine radical cations,^{15,53} which was based upon dynamics calculations on a saturated-bridged bis-bicyclic hydrazine.⁵⁴

Calculation of k_{ET} from Optically Derived ET Parameters.

Classical Marcus ET theory^{12,13} uses a two-state model having parabolic diabatic free energy surfaces that are displaced on the x coordinate, often called the electron-transfer coordinate, that includes both the internal geometry reorganization (λ_v) and the solvent reorganization (λ_s) components of the reorganization energy λ . The relative sizes of λ and the electronic interaction between the diabatic surfaces, V_{ab} , controls the shape of the ground state energy surface. When $V_{\text{ab}} < \lambda/2$, there is a double minimum on the ground state energy surface with a barrier between them of $\Delta G^* = \lambda/4 - V_{\text{ab}} + V_{\text{ab}}^2/\lambda$. The expression for the rate constant that Sutin used¹³ is eq 3,

$$k_{\text{et}} = \kappa_{\text{el}} \nu_n \exp(-\Delta G^*/RT) \quad (3)$$

where $\nu_n = c\omega_v$, the averaged vibrational modes that is the effective nuclear attempt frequency to reach the barrier. κ_{el} represents the electronic tunneling probability. Equation 3 is designed to cover rate constants ranging from the nonadiabatic region, where $\kappa_{\text{el}} = V_{\text{ab}}^2(\pi/\lambda k_B T)^{1/2}/\hbar \nu_n$ to the adiabatic region, where $\kappa = 1$. In the intermediate region, the prefactor is determined by the Landau–Zener theory developed to allow solution of the two-state model introduced by Landau, Zener, and Steckelberg in 1932 in the electronic coupling region that is chemically significant.^{55–57} Equation 3 works rather well for prediction of k_{et} as a function of temperature for 1^+ and related compounds using λ and V_{ab} obtained from Hush theory, and agreement with experiment is better when a refractive index correction is included in evaluating V_{ab} and the diabatic surfaces are allowed to vary from being perfect parabolas by including a quartic term, so that the experimental IV band is properly fit.^{14,15}

To incorporate the nuclear quantum effects, the Bixon–Jortner approach abandons the idea of an ET barrier as being important and replaces ΔG^* with Franck–Condon tunneling factors in their rate expressions. Parabolic diabatic energy surfaces are retained, but the x coordinate for these parabolas only includes the low-frequency contributions to λ that may be treated classically (usually called λ_s and identified as the solvent contribution to λ). The higher frequency components of λ , λ_v , are separated for a quantum mechanical treatment that usually uses a single “averaged” vibrational mode, ω_v , popularized for ET reactions by Jortner and co-workers,^{58,59} and leads to eqs 4a–c, called the Golden Rule equation by Closs and co-workers.⁶⁰

$$k_{\text{GR}} = (2\pi/\hbar) |V^2| \text{ (FCWD)} \quad (4a)$$

$$\text{FCWD} = (4\pi\lambda_s k_B T)^{-1/2} \sum (e^{-S} S^w/w!) \quad (4b)$$

$$\exp\{-(\lambda_s + \Delta G^\circ + w\omega_v)^2/4\lambda_s k_B T\} \quad (4b)$$

$$S = \lambda_v/\omega_v \quad (4c)$$

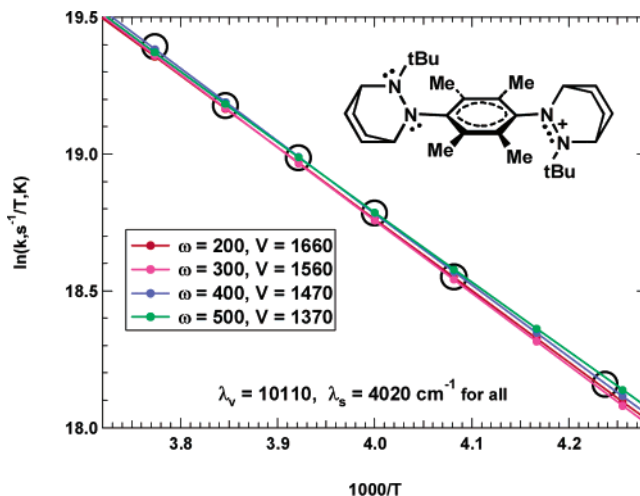


Figure 3. Eyring plots showing best fit of Zhu–Nakamura rate constant calculations to the experimental data for 1^+ in acetonitrile using the room temperature λ value.

Although eqs 4a–c have been widely used to treat ET rate constants, their use is appropriate for weak electronic coupling cases, that is, where perturbation theory is valid for V_{ab} . As V_{ab} increases, the evaluation of the ET rate constant remains a challenge because perturbation theory breaks down, which we believe is the reason for eq 4 predicting the wrong temperature dependence for 1^+ and related compounds.^{14,15,61} The classical treatment of eq 3 predicts the rate constant as a function of temperature for 1^+ and related compounds rather accurately,⁵³ but it is clear from calculations that this compound cannot be going through a classical transition state for electron-transfer because the electronic coupling would be far too large to be compatible with the observed rate constant.⁶² The appropriate electronic coupling to predict the thermal electron-transfer rate constant is that for the ground state geometry, which is that evaluated from the optical absorption spectrum using Hush theory. This observation is consistent with ET being a tunneling process, which is the assumption upon which eq 4 is based.

Most recently, Zhao et al.^{63,64} have proposed the approach to the ET on the basis of the quantum flux–flux correlation function, the transition-state theory, and the surface hopping technique. The formula is simplified to eqs 5a–b

$$k_{\text{et}} = \kappa \exp(-\Delta G^*/RT) \quad (5a)$$

$$\kappa = (2k_B T/\hbar) \sinh(\hbar\omega/2k_B T) \times$$

$$\int_0^\infty dE \exp[-(E - \Delta G^*)/k_B T] P_{\text{ZN}}(E) \quad (5b)$$

for an effectively one-dimensional mode system, where $P_{\text{ZN}}(E)$ represents the Zhu–Nakamura (ZN) nonadiabatic probability^{3–5} at a given energy E . Equation 5 represents modified classical Marcus theory that retains an electron-transfer barrier but has a different prefactor that correctly predicts the Franck–Condon factor in the nonadiabatic region and that also approaches the Marcus adiabatic ET formula in the high temperature approximation. Because the ZN formulas that overcome most of the deficiencies of Landau–Zener theory are used in eq 5b to obtain the prefactor, it incorporates the nuclear tunneling as well as the combined contribution from electron and nuclear motion. Despite some heuristic corrections to eq 3, for example, the nuclear tunneling factor is introduced with use of the parabolic approximation, the approximations in eq 3 can be significantly different from the actual solutions.

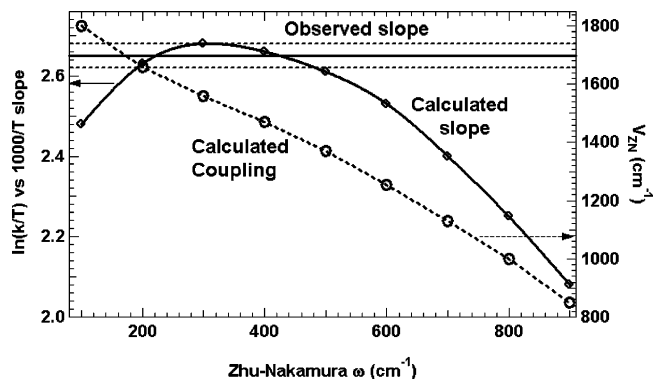


Figure 4. Eyring slopes (left axis, solid line) and electronic coupling (right axis, dashed line) for calculations compared with the experimental value of the slope for 1^+ in acetonitrile (the horizontal dotted lines show 1 standard deviation in this slope).

TABLE 2: Optical Parameters for 1^+ as a Function of Temperature^a

temp, K	E_{\max}^a	E_{quart}^b	quartic coeff ^b	μ_{12} (D)	$V_{\text{Hush}},^b \text{ cm}^{-1}$
326	14 260	14095	0.18	2.205	1040
312	14 210	14130	0.18	2.196	1037
298	14 160	14217	0.19	2.196	1038
284	14 110	14217	0.20	2.203	1044
270	14 050	14322	0.21	2.204	1049
255	13 990	14375	0.22	2.203	1050

^a From ref 32. ^b Redetermined in this work from the spectra reported in ref 32 (see text).

TABLE 3: Electronic Couplings Estimated for 1^+ Considering Temperature Variation of λ for the ESR Rate Constants Calculated Using Zhu–Nakamura Formulas

$T, \text{ K}$	$10^8 k_{\text{ESR}}, \text{ s}^{-1}$	$\lambda(T), \text{ cm}^{-1}$	$V_{\text{ZN}}, \omega = 400$	$V_{\text{ZN}}, \omega = 500$	$V_{\text{ZN}}, \omega = 600$	$V_{\text{ZN}}, \omega = 700$
265	2.64	14 227	1480	1350	1197	1017
260	2.13	14 350	1480	1348	1190	1004
255	1.76	14 370	1485	1350	1188	996
250	1.44	14 390	1489	1352	1188	988
245	1.14	14 409	1490	1352	1178	945
236	0.77	14 445	1498	1353	1174	953

Treatment of the ESR Rate Constants Using Zhu–Nakamura Formulas. The experimental rate constant data for 1^+ consists of six rate constants measured by ESR between 236 and 265 K.¹⁵ Figure 3 compares Eyring plots of the observed ESR rate constants with Zhu–Nakamura (eq 5) calculations where pairs of ω and V values that produce Eyring plots within experimental error of the ESR rate constants (shown as the black circles). These calculations were done using the partitioning of the room temperature IV band maximum in acetonitrile, taken as λ , into $\lambda_v = 10\,110 \text{ cm}^{-1}$ and $\lambda_s = 4020 \text{ cm}^{-1}$ that arose from how λ changes with solvent.⁵¹ However, other calculations showed that the results were indistinguishable if λ was not broken into vibrational and solvent components but taken as a single $14\,130 \text{ cm}^{-1}$ quantity (see Supporting Information). This result is very different from that obtained using Bixon–Jortner theory to calculate rate constants, where $S = \lambda_v/\omega_v$ is a parameter of fundamental importance, so the partitioning of λ is crucial. Calculations varying ω from 100 to 800 cm^{-1} values, also at $\lambda = 14\,130 \text{ cm}^{-1}$ are shown in Figure 4. The V value for best fit to k_{ESR} at 250 K, near the center of the range of temperatures, where accuracy in determining k_{ESR} is best, is shown as the blue circles and line (plotted on the right axis). The red circles and line show the calculated Eyring slope in the 236–265 K temperature range are plotted on the left axis. It is seen that Eyring slopes within 1 standard deviation of the observed slope

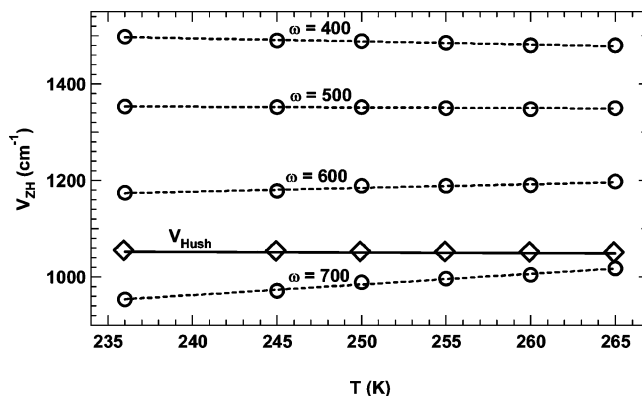


Figure 5. Circles: Plot of V_{ZH} as a function of temperature and ω obtained for the k_{ESR}, λ pairs (Table 5), chosen for best fit to k_{ESR} at 250 K. Diamonds: Plot of optically derived V_{Hush} (Table 2) as a function of temperature.

are obtained for $\omega = 200\text{--}500 \text{ cm}^{-1}$ and that the corresponding electronic coupling drops approximately linearly, by about 1 cm^{-1} in V_{ZN} per cm^{-1} change in ω over this range, from 1660 to 1370 cm^{-1} . However the series of calculations shown in Figure 4 do not take into account the fact that both λ and the optical V value, V_{Hush} , are experimentally slightly temperature sensitive,⁵³ so we will next consider the effect of allowing these quantities to vary. Table 2 shows variable temperature optical measurements, with recalculated V_{Hush} (evaluated using the dication triplet ESR-derived electron-transfer distance on the adiabatic surfaces, $d_{12} = 5.63 \text{ \AA}$,¹⁵ corresponding to the ET distance $d_{\text{ab}} = 5.71 \text{ \AA}$), employing a refractive index correction⁶⁵ and integration of the IV band to determine μ_{12} , as described recently.⁶⁶ V_{Hush} calculated in this manner decreases about $0.34 \text{ cm}^{-1}/\text{K}$ as the temperature is increased. The direction of the change seems reasonable because increasing temperature should slightly increase the average amount of twist about the C–N bonds connecting the hydrazine units to the bridge, which will decrease the electronic coupling. Instead of using the band maximum as λ , as was done previously,³² the IV band was fit more realistically, using a quartic-enhanced IV band¹⁴ along with higher energy Gaussians as needed to fit the observed spectrum, which upon analyzing substituted naphthalenes that have even more band overlap,⁶⁶ we realized will produce more realistic temperature variation of the IV band. The E_{quart} values of Table 2 were used to establish a line for $\lambda(T)$, which was used to estimate the $\lambda(T)$ values at the temperatures of the ESR data.

Table 3 shows the ESR rate constants as a function of temperature, extrapolated $\lambda(T)$ values, and Zhu–Nakamura-derived V_{ZH} values as a function of ω that best fit the rate constant, λ pairs at 250 K. As may be seen in the plot of these data in Figure 5, the slopes of the V_{ZH} values for best fit with the ESR rate constants at 250 K depend upon ω : V_{ZN} decreases $-0.64 \text{ cm}^{-1}/\text{K}$ at $\omega = 400 \text{ cm}^{-1}$ and $-0.15 \text{ cm}^{-1}/\text{K}$ at $\omega = 500$, but increases at higher ω values, $+0.77 \text{ cm}^{-1}/\text{K}$ at $\omega = 600 \text{ cm}^{-1}$ and $+2.19 \text{ cm}^{-1}/\text{K}$ at $\omega = 700 \text{ cm}^{-1}$. The optically derived V_{Hush} decreases slightly as temperature increases, slope $-0.13 \text{ cm}^{-1}/\text{K}$. This is reasonable because electronic coupling depends upon overlap of the charge-bearing units with the bridge, making V about proportional to $\cos \phi$ at each of the CN connecting bonds, and we expect the average value of ϕ to increase slightly as the temperature increases. Although the temperature sensitivity of V_{ZN} is closer to that for V_{Hush} at $\omega = 500 \text{ cm}^{-1}$, the size of V_{ZN} is closer to V_{Hush} near about $\omega = 660\text{--}680 \text{ cm}^{-1}$, depending upon temperature. It is not obvious how sensitive ω should be to temperature.

However, a smaller ω than the resonance Raman ω_v fits the ESR and optical data better. This is expected because a single ω eq 5 calculation must include the low-frequency solvent modes as well as higher frequency internal vibration modes. Newton and Sutin have discussed the effective frequency arising from intramolecular and solvent modes.^{67,68} Following them, the effective frequency used in eq 5 is written as eq 6

$$\omega_{\text{eff}}^2 = (\omega_v^2 \lambda_v + \omega_s^2 \lambda_s) / \lambda \quad (6)$$

where ω_s is the solvent rotational frequency. Dmitry Matyushov (Arizona State)⁶⁹ derived an expression using a quasi-classical approximation that gives a somewhat different expression for the effective ω value, as shown in eq 7

$$\omega'_{\text{eff}} \approx (\sum_q \lambda(q) \omega(q) + \lambda_s / \tau_L) / \lambda \quad (7)$$

These expressions explicitly show that ω is always smaller than ω_v . Using recent dielectric data for acetonitrile⁷⁰ as summarized by Matyushov⁷¹ produces $\tau_L^{-1} = 185 \text{ cm}^{-1}$. Using this value as ω_s in (6) with the resonance Raman λ_v of 9248 cm^{-1} gives $\omega_{\text{eff}} = 574 \text{ cm}^{-1}$, while (7) produces a lower value, $\omega'_{\text{eff}} = 414 \text{ cm}^{-1}$. Thus the Newton–Sutin estimate of ω (eq 6) is consistent with a V_{ZN} at 250 K of about 1230 cm^{-1} , while the Matyushov estimate with V_{ZN} of about 1470 cm^{-1} , both of which are larger than the Hush estimate derived from the optical spectra of about 1050 cm^{-1} . Nevertheless, we consider these results rather good agreement for the quite independent estimations of the effective ω using the temperature variation of the ESR rate constant as analyzed by ZN theory and the resonance Raman spectrum. Thus Marcus–Hush analysis of the optical data to evaluate λ and V_{Hush} produces a larger value (ca. 670 cm^{-1}) than the resonance Raman-derived fractionation of λ_v into its mode-by-mode components (414 or 575 cm^{-1} , depending on whether eq 6 or 7 is used to estimate the effective ω value.

Summary

A resonance Raman study revealed 11 modes excited by irradiation into the intervalence band of 1^+ . They range from 435 to 1550 cm^{-1} , and their incremental contributions sum to $\lambda_v^{\text{sym}} = 9250 \text{ cm}^{-1}$. Low-frequency bending and twisting motions predominate in causing this vibrational reorganization energy: 67% of λ_v^{sym} arises from modes $\leq 506 \text{ cm}^{-1}$ and 86% from those $\leq 748 \text{ cm}^{-1}$. The value of ω_v obtained from the resonance Raman data is 697 cm^{-1} , which produces a predicted single mode effective ω value of 574 and 414 cm^{-1} using eqs 6 and 7, respectively. The Zhu–Nakamura formulas have been used obtaining ω, V combinations that are consistent with the experimental temperature dependence of the ESR-derived electron-transfer rate constant and optical λ value. In contrast to using Bixon–Jortner theory, separation of λ into its λ_s and λ_v components does not significantly affect the ω, V pairs that fit a given rate constant. Using the Zhu–Nakamura preexponential factor of eq 5 gives good agreement for the ESR rate constants using an ω value that is close to those estimated from the resonance Raman spectroscopic data but requiring a slightly higher electronic coupling than V_{Hush} .

Acknowledgment. This work was made possible by grants from the National Science Foundation, CHE-0240197 (S.F.N.) and CHE-0507929 (J.I.Z.), and NSFC-20473080 (Y.Z.).

Supporting Information Available: Absolute and normalized intensity data for the resonance Raman of 1^+ , additional Eyring plot comparisons of experimental and calculated rate

constant data, and the data plotted in Figure 4. This material is available free of charge via the Internet at <http://pubs.acs.org>.

References and Notes

- (1) Robin, M. B.; Day, P. *Adv. Inorg. Radiochem.* **1967**, *10*, 247–422.
- (2) Creutz, C.; Taube, H. *J. Am. Chem. Soc.* **1969**, *91*, 3988–9.
- (3) Creutz, C. *Prog. Inorg. Chem.* **1983**, *30*, 1–73.
- (4) Crutchley, R. J. *Adv. Inorg. Chem.* **1994**, *41*, 273–325.
- (5) Hush, N. S. *Prog. Inorg. Chem.* **1967**, *8*, 391–444.
- (6) Hush, N. S. *Coord. Chem. Rev.* **1985**, *64*, 135–157.
- (7) For the early history of radical ion studies, see: Roth, H. D. *Tetrahedron* **1986**, *42*, 6097–6100.
- (8) We believe that Cowan and co-workers first pointed out an all-organic Class III intervalence system, tetrathiofulvalene radical cation: Cowan, D. O.; LeVanda, C.; Park, J.; Kaufman, F. *Acc. Chem. Res.* **1973**, *6*, 1–7.
- (9) Nelsen, S. F.; Chang, H.; Wolff, J. J.; Adamus, J. J. *Am. Chem. Soc.* **1993**, *115*, 12276–12289.
- (10) Nelsen, S. F.; Ismagilov, R. F.; Powell, D. R. *J. Am. Chem. Soc.* **1996**, *118*, 6313–6314.
- (11) For a recent review see: Nelsen, S. F. *Adv. Phys. Org. Chem.* **2006**, *41*, 183–215.
- (12) Marcus, R. A. *J. Chem. Phys.* **1956**, *24*, 966–978.
- (13) Sutin, N. *Prog. Inorg. Chem.* **1983**, *30*, 441–499.
- (14) Nelsen, S. F.; Ismagilov, R. F.; Trieber, D. A., II *Science* **1997**, *278*, 846–849.
- (15) Nelsen, S. F.; Ismagilov, R. F.; Powell, D. R. *J. Am. Chem. Soc.* **1997**, *119*, 10213–10222.
- (16) Yang, Y. Y. and Zink, J. I. *J. Am. Chem. Soc.* **1984**, *106*, 1500.
- (17) Zink, J. I. *Coord. Chem. Rev.* **1985**, *64*, 93.
- (18) (a) Doorn, S. K.; Hupp, J. T. *J. Am. Chem. Soc.* **1989**, *111*, 1142–1144. (b) Doorn, S. K.; Hupp, J. T. *J. Am. Chem. Soc.* **1989**, *111*, 4704–4712.
- (19) Henary, M.; Zink, J. I. *J. Am. Chem. Soc.* **1989**, *111*, 7407.
- (20) Shin, K. S.; Clark, R. J. H.; Zink, J. I. *J. Am. Chem. Soc.* **1990**, *112*, 3754.
- (21) Shin, K. S.; Clark, R. J. H.; Zink, J. I. *J. Am. Chem. Soc.* **1990**, *112*, 7148.
- (22) Kim Shin, K.-S.; Zink, J. I. *J. Am. Chem. Soc.* **1990**, *112*, 7148.
- (23) Doorn, S. K.; Hupp, J. T.; Porterfield, D. R.; Campion, A.; Chase, D. B. *J. Am. Chem. Soc.* **1990**, *112*, 4999–5002.
- (24) Doorn, S. K.; Blackburn, R. L.; Johnson, C. S.; Hupp, J. T. *Electrochim. Acta* **1991**, *36*, 1775–1785.
- (25) Blackburn, R. L.; Johnson, C. S.; Hupp, J. T. *J. Am. Chem. Soc.* **1991**, *113*, 1060–1062.
- (26) (a) Petrov, V.; Hupp, J. T.; Mottley, C.; Mann, L. C. *J. Am. Chem. Soc.* **1994**, *116*, 2171. (b) Lu, H.; Petrov, V.; Hupp, J. T. *Chem. Phys. Lett.* **1995**, *235*, 521–527.
- (27) Wootton, J. L.; Zink, J. I. *J. Phys. Chem.* **1995**, *99*, 7251.
- (28) Henary, M.; Wootton, J. L.; Khan, S. I.; Zink, J. I. *Inorg. Chem.* **1997**, *36*, 796.
- (29) Hanna, S. D.; Zink, J. I. *Inorg. Chem.* **1996**, *35*, 297.
- (30) Zink, J. I. *Coord. Chem. Rev.* **2001**, *211*, 69.
- (31) Blackburn, R. L.; Johnson, C. S.; Hupp, J. T.; Bryant, M. A.; Sobocinski, R. L.; Pemberton, J. E. *J. Phys. Chem.* **1991**, *95*, 10535–10537.
- (32) Meyers, A. B. *Chem. Phys.* **1994**, *180*, 215.
- (33) Godbout, J. T.; Pietrzykowski, M. D.; Gould, I. R.; Goodman, J. T.; Kelly, A. M. *J. Phys. Chem. A* **1999**, *103*, 3876–3883.
- (34) Kelly, A. M. *J. Phys. Chem. A* **1999**, *103*, 6891–6903.
- (35) Meyers, A. B. *Chem. Rev.* **1996**, *96*, 911–926.
- (36) Doorn, S. K.; Blackburn, R. L.; Johnson, C. S.; Hupp, J. T. *Electrochim. Acta* **1991**, *36*, 1775–1785.
- (37) Blackburn, R. L.; Johnson, C. S.; Hupp, J. T. *J. Am. Chem. Soc.* **1991**, *113*, 1060–1062.
- (38) Bailey, S. E.; Zink, J. I.; Nelsen, S. F. *J. Am. Chem. Soc.* **2003**, *125*, 5939–5947.
- (39) Szeghalmi, A. V.; Erdmann, M.; Engel, V.; Schmidt, M.; Amthor, S.; Kriegisch, V.; Nöll, G.; Stahl, R.; Lambert, C.; Leusser, D.; Stalke, D.; Zabel, M.; Popp, J. *J. Am. Chem. Soc.* **2004**, *126*, 7834–7845.
- (40) Lockard, J. V.; Zink, J. I.; Trieber, D. A., II; Konradsson, A. E.; Weaver, M. N.; Nelsen, S. F. *J. Phys. Chem. A* **2005**, *109*, 1205–1215.
- (41) Lockard, J. V.; Valverde, G.; Neuhauser, D.; Zink, J. I.; Luo, Y.; Weaver, M. N.; Nelsen, S. F. *J. Phys. Chem. A* **2006**, *110*, 57–66.
- (42) Lee, S.-Y.; Heller, E. J. *J. Chem. Phys.* **1979**, *71*, 4777.
- (43) Heller, E. J. *Acc. Chem. Res.* **1981**, *14*, 368–375.
- (44) Heller, E. J.; Sundberg, R. L.; Tannor, D. *J. Phys. Chem.* **1982**, *86*, 1822–1833.
- (45) Zink, J. I.; Shin, K.-S. K. In *Advances in Photochemistry*; Wiley: New York, 1991; Vol. 16, p 119.
- (46) Shin, K.-S. K.; Zink, J. I. *Inorg. Chem.* **1989**, *28*, 4358.
- (47) Myers Kelley, A. *J. Phys. Chem. A* **1999**, *103*, 6891.

- (48) Myers, A. B. *Chem. Rev.* **1996**, *96*, 911.
- (49) Myers, A. B. *Acc. Chem. Res.* **1997**, *30*, 519.
- (50) Myers, A. B. In *Laser Techniques in Chemistry*; Wiley: New York, 1995; Vol. 23, p 325.
- (51) Nelsen, S. F.; Trieber, D. A., II.; Ismagilov, R. F.; Teki, Y. *J. Am. Chem. Soc.* **2001**, *123*, 5684.
- (52) Equation 45 of ref 13.
- (53) Nelsen, S. F.; Ismagilov, R. F.; Gentile, K. E.; Powell, D. R. *J. Am. Chem. Soc.* **1999**, *121*, 7108–7114.
- (54) Nelsen, S. F. *J. Am. Chem. Soc.* **1996**, *118*, 2047–2058.
- (55) Zhu, C.; Nakamura, H. *J. Chem. Phys.* **1994**, *101*, 10630–10647.
- (56) Zhu, C.; Nakamura, H. *J. Chem. Phys.* **1995**, *102*, 7448–7462.
- (57) Zhu, C.; Teranishi, Y.; Nakamura, H. *Adv. Chem. Phys.* **2001**, *117*, 127–233.
- (58) Ulstrup, J.; Jortner, J. *J. Chem. Phys.* **1975**, *63*, 4358–4368.
- (59) Bixon, M.; Jortner, J. *Adv. Chem. Phys.* **1999**, *106*, 35–202.
- (60) (a) Closs, G. L.; Miller, J. R. *Science* **1988**, *240*, 440–448. (b) Liang, N.; Miller, J. R.; Closs, G. L. *J. Am. Chem. Soc.* **1989**, *111*, 8740–8741. (c) Liang, N.; Miller, J. R.; Closs, G. L. *J. Am. Chem. Soc.* **1990**, *112*, 5353–5354.
- (61) A more complicated, double sum form of eq 4 was actually used for these intervalence compounds,^{14,15} which is necessary because $\Delta G^\circ = 0$ and the “forward” rate is the same as the “back” rate. A still more complex, Bessel function form of eq 4 has been proposed to correct for ω_v being greater than $2kT$ (ref 59, eq 5.28) but to our knowledge is seldom used by experimentalists. We do not think its use would improve agreement with our experimental data significantly. The principal problem with eq 4, it seems to us, is that S is not an important parameter for this compound.
- (62) Blomgren, F.; Larsson, S.; Nelsen, S. F. *J. Comput. Chem.* **2001**, *22*, 655.
- (63) Zhao, Y.; Mil'nikov, G.; Nakamura, H. *J. Chem. Phys.* **2004**, *121*, 8854–8860.
- (64) Zhao, Y.; Nakamura, H. *J. Theor. Comput. Chem.* **2006**, *5*, 299–306.
- (65) We note that not including the refractive index correction (which Hush never used) increases what we call V_{Hush} by about 100 cm^{-1} for these data, which it will be noted below would improve agreement with the Zhu–Nakamura calculations.
- (66) Nelsen, S. F.; Konradsson, A. E.; Teki, Y. *J. Am. Chem. Soc.* **2006**, *128*, 2902–2910.
- (67) Newton, M. D.; Sutin, N. *Annu. Rev. Phys. Chem.* **1984**, *35*, 437–480.
- (68) Sutin, N. *Prog. Inorg. Chem.* **1983**, *30*, 441–499.
- (69) Matyushov, Dmitry V. Private communications, August 2006.
- (70) Asaki, M. L. T.; Redondo, A.; Zawodzinski, T. A.; Taylor, A. J. *J. Chem. Phys.* **2002**, *116*, 10377–10385.
- (71) Matushov, D. V. *J. Chem. Phys.* **2005**, *122*, 044502.1–11.